

Consistently modeling the combined effects of temperature and concentration on nitrate uptake in the ocean

S. Lan Smith¹

Received 6 February 2011; revised 24 August 2011; accepted 27 August 2011; published 16 November 2011.

[1] Considerable uncertainty remains about the combined effects of multiple limiting factors on oceanic phytoplankton, which constitute the base of the marine food web and mediate biogeochemical cycles of carbon and nutrients. I apply Bayesian statistical analysis to disentangle the combined effects of temperature and concentration on uptake of the important nutrient nitrate as measured by oceanic field experiments. This provides consistent estimates of temperature sensitivities for the maximum uptake rate and affinity (initial slope), the two parameters which define the shape of the uptake-concentration curve. No evidence is found that the temperature sensitivities of these two parameters differ, which implies that half-saturation constants, as commonly obtained by fits of the Michaelis-Menten (MM) equation, should be independent of temperature. This explains the robust relationship between half-saturation values and ambient nitrate concentration observed in compilations of data from diverse studies of uptake in marine and freshwater environments. Compared to the MM kinetics as applied in most large-scale models, accounting for a physiological trade-off between maximum uptake rate and affinity: (1) yields a more consistent model, which better describes observed changes in the shape of the uptake-concentration curve, and (2) implies a significantly greater inferred temperature sensitivity for nitrate uptake. These findings impact our understanding of how marine ecosystems and biogeochemical cycles will respond to climate change and anthropogenic nutrient inputs, both of which are expected to alter the relationship between nutrient concentrations and temperature in the near-surface ocean.

Citation: Smith, S. L. (2011), Consistently modeling the combined effects of temperature and concentration on nitrate uptake in the ocean, *J. Geophys. Res.*, 116, G04020, doi:10.1029/2011JG001681.

1. Introduction

[2] Accurate representations of the temperature dependence of biological processes are essential if we are to understand the direct effects and associated feedbacks of natural physical variability, anthropogenic nutrient inputs and climate change on ecosystems and biogeochemical cycles. Most of our current knowledge about the temperature dependence of phytoplankton processes comes from laboratory experiments with single-species cultures. Few data sets from field studies even exist which allow directly testing whether those results can be extrapolated to the real ocean. However, accounting for the combined effects of multiple limiting factors implies different patterns for growth [Moisan *et al.*, 2002] and nutrient uptake [Smith, 2010] by phytoplankton in the ocean.

[3] *Eppley* [1972] estimated the temperature dependence of maximum potential growth rate for phytoplankton by fitting to the “top of the data” (fastest growth rate measured

at each temperature) using a compilation of data from many single-species culture experiments, reasoning that this would exclude the effects of other potential limiting factors such as nutrients and light. Statistical analysis of a more extensive data set has recently confirmed this exponential dependence, with slight modification of its parameters [Bissinger *et al.*, 2008]. However, *Eppley* [1972] noted that this overall exponential dependence contrasts with the steep decrease in growth rate typically observed for any single species above its species-specific optimal temperature, T_o . Recently some complex large-scale models do resolve distinct values of T_o for different species [e.g., *Follows et al.*, 2007] or functional types [e.g., *LeQuere et al.*, 2005]. However, such models are too computationally demanding for direct use in long-term studies of biogeochemical cycles and climate, although they may provide valuable information and parameterizations that can be useful for long-term studies with other models. Therefore, many large-scale models assume exponential temperature dependence, multiplied by other limiting factors, for nutrient uptake, growth and other biological processes [e.g., *Fasham et al.*, 1993; *Aumont et al.*, 2003; *Kishi et al.*, 2007]. The best justification for this assumption is that it represents the ecological dependence, under the assumption that at ambient environmental temperature, T_a ,

¹Environmental Biogeochemical Cycles Research Program, RIGC, JAMSTEC, Yokohama-shi, Japan.

the dominant species will have optimal temperature $T_o = T_a$ [Eppley, 1972]. On the other hand, many oceanic biogeochemical models [e.g., Yamanaka and Tajika, 1996; Parekh et al., 2005; Marinov et al., 2008] assume no temperature dependence for nutrient uptake.

[4] Here I test assumptions about the combined effects of temperature and nutrient concentration on uptake rate against an extensive data set for nitrate uptake as measured in field experiments [Harrison et al., 1996]. This addresses the overall (ecological) temperature dependence across the various species that dominate at different locations and seasons, not the dependence for any given species. I test the hypothesis that the parameters of uptake kinetics (i.e., the shape of the uptake-concentration curve), as determined in typical short-term incubation experiments, depend on both temperature and ambient nutrient concentration. I consider two representations of the dependence of these uptake parameters on concentration: (1) the assumption of fixed physiology inherent in the widely-applied Michaelis-Menten (MM) kinetics, which assumes no dependence of these parameters on ambient nutrient concentration, and (2) the recently developed Optimal Uptake (OU) kinetics, based on a physiological trade-off between maximum uptake rate and affinity for nutrient (assuming that physiology and hence the shape of the uptake-concentration curve depend on the ambient nutrient concentration). I apply the Adaptive Metropolis algorithm [Haario et al., 2001; Laine, 2008], an automatic Bayesian statistical method, to assess how well each set of assumptions agrees with the data set as a whole. This reveals that OU kinetics: (1) better describes the patterns of variation for the uptake parameters, which depend on both temperature and nutrient concentration, and (2) implies a greater sensitivity of these parameters to temperature than does MM kinetics. It further reveals no evidence that the temperature sensitivities of maximum uptake rate and affinity differ, which explains the lack of any consistent dependence of MM half-saturation constants on temperature (at least at the large scale).

2. Methods

2.1. Theory

[5] For phytoplankton and other microorganisms, the Michaelis-Menten (MM) equation is most commonly applied to describe the dependence of uptake rate on nutrient concentration [Dugdale, 1967; Harrison et al., 1996]:

$$V_{MM} = \frac{V_{\max}S}{K_s + S} \quad (1)$$

where V_{MM} is the uptake rate, S is the nutrient concentration, and K_s is the MM half-saturation constant for nutrient S . This equation is often combined with Arrhenius-type [Goldman and Carpenter, 1974] or similar exponential [Eppley, 1972] temperature dependence for V_{\max} .

[6] Compared to equation (1), Affinity-based kinetics provides a more natural and theoretically well-founded representation of uptake [Aksnes and Egge, 1991]. Affinity, A , is defined as the initial slope of rate versus con-

centration at low nutrient concentrations [Healey, 1980], so that:

$$V_A = \frac{V_{\max}AS}{V_{\max} + AS} \quad (2)$$

Aksnes and Egge [1991] showed that MM kinetics is equivalent to affinity-based kinetics under the assumption of fixed physiology (no acclimation in response to changing nutrient concentrations); i.e., for constant V_{\max} and A , equation (2) is mathematically equivalent to equation (1). Furthermore, equation (2) with temperature dependent V_{\max} and A is equivalent to equation (1) with temperature dependent V_{\max} and K_s . If V_{\max} and A share identical temperature dependence, K_s must be independent of temperature.

[7] However, experiments with various single-species cultures have found temperature dependent K_s for uptake of nitrogen, phosphorus and silicon [Eppley et al., 1969; Dauta, 1982]. Therefore, I examine the possibility of distinct temperature sensitivities for V_{\max} and A , by defining energies of activation, $E_{a,V}$ and $E_{a,A}$, respectively, such that:

$$V_{\max} = V_{\max,r} \exp\{-(1/T - 1/T_r)E_{a,V}/R\} \quad (3a)$$

$$A = A_r \exp\{-(1/T - 1/T_r)E_{a,A}/R\} \quad (3b)$$

where T is temperature in K, R is the gas constant, and $V_{\max,r}$ and A_r are the values of V_{\max} and A , respectively, at reference temperature T_r . If $E_{a,A} = E_{a,V}$, one set of Arrhenius terms cancels out after substitution into equation (2), leaving only one Arrhenius term in the numerator, which is equivalent to the widely applied assumption of temperature dependence only for V_{\max} [Goldman and Carpenter, 1974].

[8] Optimal Uptake (OU) kinetics extends equation (2) to include a physiological trade-off, whereby phytoplankton allocate internal resources to increase either V_{\max} or A , at the expense of reducing the other [Pahlow, 2005; Smith et al., 2009]. V_0 and A_0 are defined as the potential maximum values of V_{\max} and A , respectively, and their actual values are determined by physiological acclimation to the ambient concentration of growth-limiting nutrient. The data examined here [Harrison et al., 1996] were from typical short-term uptake experiments [Harrison et al., 1989], in which a series of incubations with graded nutrient additions is conducted for each sample taken from water having ambient nutrient concentration, S_a . Assuming that phytoplankton were pre-acclimated to S_a , OU kinetics gives the following equations for the dependence on S_a of affinity-based parameters, as measured by short-term experiments during which the phytoplankton do not have time to acclimate [Smith et al., 2009; Smith, 2010]:

$$V_{\max} = \frac{\sqrt{\frac{A_0 S_a}{V_0}}}{1 + \sqrt{\frac{A_0 S_a}{V_0}}} V_0 \quad (4)$$

$$A = \frac{1}{1 + \sqrt{\frac{A_0 S_a}{V_0}}} A_0 \quad (5)$$

Note that S_a , the ambient concentration in the ocean, is not the concentration S in the short-term incubation experiments using graded nutrient additions. This predicts that such short-term experiments will measure values of V_{\max} that increase with S_a and values of A that decrease with increasing S_a . For temperature dependence with OU kinetics I apply Arrhenius terms for V_0 and A_0 , respectively, by defining $E_{a,V}$, $E_{a,A}$, $V_{0,r}$ and $A_{0,r}$, exactly analogous to the above treatment for V_{\max} and A with MM kinetics equations (3a) and (3b).

2.2. Data

[9] Data were those of *Harrison et al.* [1996] as rearranged by *Smith* [2010] to match observed ambient temperatures and nitrate concentrations to the reported values of V_{\max} ($n = 60$) and K_s ($n = 48$) as obtained from their short-term (~3h) incubation experiments. At each of the locations, which covered the North Atlantic ocean, graded nutrient additions were made to separate bottles containing sampled seawater, which were then incubated ship-board at ambient temperature in order to measure nutrient uptake rates. They calculated parameters of the MM equation for nutrient uptake by fitting to the data so obtained locally, i.e., for the set of experiments conducted at each location, respectively. I calculate values of affinity as $A = V_{\max}/K_s$. For the set of short-term experiments conducted using each ambient water sample, respectively, the MM equation described the shape of the uptake response well, albeit with different values of V_{\max} and K_s for different water samples [*Harrison et al.*, 1996]. Either equation (1) or equation (2) describes this same shape, the only difference being whether K_s or A is employed.

2.3. Fitting

2.3.1. General Approach

[10] The Adaptive Metropolis (AM) algorithm [*Haario et al.*, 2001; *Laine*, 2008] yields a consistent Bayesian statistical interpretation of the data set as a whole, providing a way to disentangle the combined effects of temperature and nutrient concentration. I chose to fit the affinity-based equation (2) to the data, because this equation allows a concise representation of both MM and OU kinetics, whereas expressing OU kinetics in terms of K_s using equation (1), although possible, is cumbersome and counter-intuitive.

[11] Two cases are examined: (1) the ‘Affinity model’ assuming no physiological acclimation (equivalent to MM kinetics) and (2) the ‘OU model’ assuming physiological acclimation according to OU kinetics. Arrhenius-type temperature dependence was assumed for maximum uptake rate and affinity, respectively.

[12] For the Affinity model, the temperature dependent expressions for V_{\max} and A were fitted to the respective data values, using the corresponding values of ambient temperature as independent variables. For OU kinetics, the temperature dependent expressions for V_0 and A_0 were substituted into the short-term approximations for their dependence on ambient nutrient concentration, equations (4) and (5), respectively. The resulting equations were fitted to the data in the same way as for the Affinity model.

2.3.2. Adaptive Metropolis Algorithm

[13] The Adaptive Metropolis (AM) algorithm [*Haario et al.*, 2001; *Laine*, 2008], including Gibbs sampling to estimate the distribution of the standard error (variance) of each observation type [*Laine*, 2008], was used to fit each set of equations to the data. This algorithm is for the most part automatic and non-parametric; i.e., there are few arbitrary constants to be adjusted by the user. This provides a consistent comparison of each model, respectively, with the data set as a whole.

[14] In this application, Gibbs sampling provides weights for each data type, based on the mismatch between model and data, so that the ensemble of the fitted model output (posterior distribution) matches the distribution of the data. Specifically, if the model-data mismatch (residuals) for each data type o is a Normally (Gaussian) distributed random variable with mean zero and variance σ_o and the prior estimate of $1/\sigma_o^2$ is assumed to have a Gamma distribution, then the conditional distribution for each $1/\sigma_o^2$ (given the data and model) is also a Gamma distributed random variable [*Carlin and Louis*, 1996; *Gelman et al.*, 2004]. Here Gibbs sampling exploits this property, called conjugacy of the prior and conditional distributions, to sample the posterior distribution of $1/\sigma_o^2$ based on its prior estimate together with information about the distribution of model-data mismatch, which comes from the unweighted sum of squared residuals [*Carlin and Louis*, 1996, chapter 5; *Gelman et al.*, 2004, chapter 14].

[15] Output includes the sampled distribution of values for each parameter value fitted and distributions of the standard errors for each data type. Combining these gives the predicted range within which observations should lie, assuming the model is correct [*Gelman et al.*, 2004; *Laine*, 2008].

2.3.3. Likelihood Function

[16] The likelihood is calculated as in work by *Laine* [2008], based on the probability density function of the Gaussian distribution. It includes a prior component (for deviations of parameter values from their prior expected values) and a term based on the sum of squared difference between the model and data. The log likelihood is thus:

$$\log_e L = \frac{-\log_e((2\pi)^{n_p}|C_p|)}{2} - \frac{\delta_p^T C_p^{-1} \delta_p}{2} + \sum_o \left(-N_o \log_e(\sigma_o \sqrt{2\pi}) - \frac{SS_o(\theta)}{2\sigma_o^2} \right) \quad (6)$$

where C_p is the prior covariance matrix (uncertainty in the prior estimates), n_p is the number of parameters fitted, $\delta_p = \theta - \eta$ is the vector of deviations of parameter values θ from their prior values η , N_o is the number of data points for each observation type o , and SS_o is the unweighted sum of squared errors for data type o . Previous studies found that for fits to these data a log transformation is required to make the distribution of residuals approximately Gaussian (Normal) [*Smith et al.*, 2009; *Smith*, 2010]. Therefore, SS_o is calculated as:

$$SS_o = \sum_{i=1}^{N_o} (\log_{10} y_i - \log_{10} f(x_i, \theta))^2 \quad (7)$$

where y_i is the i th observed value (here, of either V_{\max} or A) and $f(x_i, \theta)$ is the modeled value as a function of the corresponding independent variables x_i (in this case, ambient temperature and nitrate concentration) and the parameter values θ .

2.3.4. Tests of the Algorithm and Robustness of Results

[17] Identical twin tests confirmed that the algorithm functions correctly and is able to constrain the fitted parameters based on this data set. Fits to reduced data sets confirmed that the complete data set is more than sufficient to draw the conclusions herein. Methods and results are described in the auxiliary material.¹

2.3.5. Model Selection

[18] As in other Bayesian methods, the likelihood provides a relative measure of goodness of fit, and the Akaike Information Criterion (AIC) [Akaike, 1974] further accounts for the trade-off between bias and variance (roughly interpretable as accuracy versus complexity) when comparing models having different numbers of parameters. Thus application of AIC to compare models in a Bayesian context is analogous to the application of ANOVA in a frequentist context to compare linear regression models having different numbers of parameters. Here I calculate AICc, which is the AIC corrected for the effects of sample size [Burnham and Anderson, 1998; Anderson et al., 2000], using the ensemble mean log likelihood ($\log \bar{L}$) for each fitted model, respectively:

$$AICc = -2 \log \bar{L} + 2p + \frac{2p(p+1)}{N-p-1} \quad (8)$$

where p is the number of parameters fitted for each model, respectively, and N is the total number of observations.

[19] AIC provides only a relative comparison of models; i.e., its absolute value for any particular model is not meaningful, but only differences between models. The model with the lowest AIC is best, and differences in AIC for each mode, m , are calculated as:

$$\Delta_{AIC,m} = AIC_m - \min_{i \leq M} (AIC_i) \quad (9)$$

where ‘min’ denotes the minimum value over the total number of models considered (M). Although $\Delta_{AIC,m}$ alone can be taken as an approximate measure of the relative support for model m compared to the best model, a quantitative measure in terms of relative probability (of each model, respectively, given the observations) is provided by the Akaike weights [Burnham and Anderson, 1998; Anderson et al., 2000]:

$$w_m = \frac{\exp\left(\frac{-\Delta_{AIC,m}}{2}\right)}{\sum_i^M \exp\left(\frac{-\Delta_{AIC,i}}{2}\right)} \quad (10)$$

Here I adopt the criteria $w_m > 0.95$ for accepting model m , and conversely $w_m < 0.05$ for rejection. This is not a hypothesis test as widely applied in frequentist statistics, but instead a relative ranking of the probabilities of all models considered given the observations [Anderson et al.,

2000]. As an alternative, the Bayesian Information Criterion (BIC) could instead be used to calculate these weights, which would tend to favor more parsimonious models more strongly than does the AIC [Schwarz, 1978; Congdon, 2001].

2.3.6. Parameters for the Algorithm

[20] The prior covariance matrix, C_p , for parameters was chosen not to be very restrictive, by assuming a coefficient of variation of 2.0 for each parameter estimate, respectively. Thus, the diagonal element (variance) corresponding to each parameter was assumed to be the square of double the prior estimate of that parameter. Non-diagonal terms were taken to be zero (no cross-correlations). Prior estimates for temperature sensitivity, E_a/R , were taken as 5.7×10^3 K, which for a 10°C increase in temperature from 283 K to 293 K corresponds to a doubling of rate. Prior estimates for V_{\max} and A at the reference temperature, $T_r = 293$ K, were taken as the maximum observed values of each parameter, respectively.

[21] For the Gibbs sampling [Laine, 2008], parameter n_0 , which represents the prior uncertainty of observations, was taken as unity, and parameter S_0 , the prior mean for each σ , was taken as 0.01 based on trial fits. The results of fits were not sensitive to the specific choice of these parameters for any $S_0 \lesssim 1$. (For larger values of S_0 the fits were not constrained because the resulting large values of σ gave very low weights to the data.) Because the sum of squares is calculated in log space as per equation (7) above, the algorithm samples the distribution of standard errors in log space as well.

2.3.7. Numerical Calculations

[22] Uniform (0, 1) pseudo-random numbers were generated using the Mersenne twister algorithm, as originally coded by Takuji Nishimura, in 1997, and later translated to FORTRAN90 by Richard Woloshyn, in 1999. From these the Gaussian (Normal) pseudo-random numbers, multivariate Gaussian pseudo-random numbers, and Gamma-distributed pseudo-random numbers needed for the AM algorithm were generated using the algorithms of Gentle [2003], which I coded into FORTRAN90. Cholesky decompositions and matrix inversions were calculated using, respectively, the CHOLSKY [Healy, 1968b] and SYMINV [Healy, 1968a] routines, as coded into FORTRAN90 by John Burkardt, in 2008.

3. Results

3.1. Correlation of Temperature and Nitrate Concentration

[23] Ambient values of observed temperature and nitrate concentration are strongly and significantly negatively correlated in this data set (Figure 1). Such negative relationships are a general feature of the near-surface ocean, although they differ quantitatively with location [Silió-Calzada et al., 2008]. Smith [2010] found a similar negative relationship between temperature and nitrate concentration in the data set by Kanda et al. [1985] from the North Pacific.

3.2. Distinct Versus Identical Temperature Sensitivities

[24] Fits of the Affinity-based and OU equations for kinetic parameters, assuming distinct temperature sensitivities for V_{\max} and A (Figure 2) resulted in lower log

¹Auxiliary materials are available in the HTML. doi:10.1029/2011JG001681.

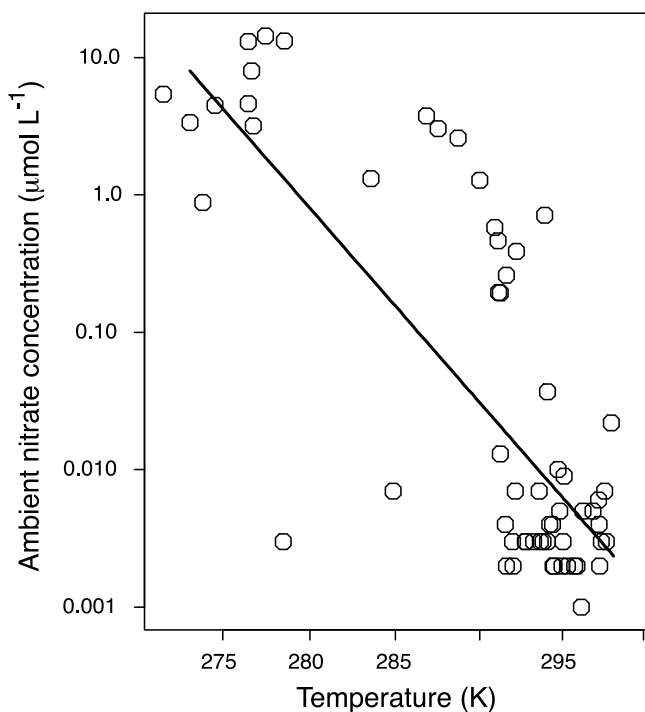


Figure 1. Relationship between observed ambient temperature (T) and nitrate concentration ($[\text{NO}_3]$) for the data set of Harrison *et al.* [1996]. The line is the linear log-log regression: $\log[\text{NO}_3] = 277 - 92.8\log T$ ($r^2 = 0.60$, $F = 85.5$, $n = 60$, $p < 10^{-12}$).

likelihoods (Table 1) than fits assuming the same temperature sensitivities (for either model, respectively). This is because increasing the number of parameters reduces the likelihood slightly through the prior contribution, which accounts for deviations of parameter values from their prior estimates. Values of Akaike Information Criteria (AIC) [Akaike, 1974] differ even more, because AIC accounts for the added uncertainty associated with the additional parameter required to account for distinct temperature sensitivities.

[25] The models with distinct temperature sensitivities for V_{\max} and A both have probabilities less than 0.01 based on the Akaike weights (Table 2) and are therefore rejected. Thus there is no evidence that the temperature sensitivities of V_{\max} and A differ, and therefore no evidence that K_s depends on temperature in this data set. Note that here I address the overall (ecological) temperature dependence across the various species that dominate at different locations and seasons, and not the dependence for any given species.

[26] The OU model assuming the same temperature sensitivity for V_{\max} and A has an Akaike weight, $w > 0.95$ (Table 2), and is therefore accepted as the model which best agrees with the observations. For the models differing only in the assumption of identical versus distinct temperature sensitivities for V_{\max} and A , results differ most for A in the model assuming no physiological trade-off (Figure 2c versus Figure 3c) and for the resulting values of K_s (Figure 2e versus Figure 3e). The Affinity model fits the observed data by making the temperature sensitivity of A much greater than that of V_{\max} , which results in a steep decrease in K_s with increasing temperature (Figure 2e). Fits to only the data

for $T > 285$ K (not shown) give the same pattern with a similarly strong temperature sensitivity for A , confirming that this is not a result only of the relatively few values of affinity at low temperatures.

3.3. Physiological Trade-Off Versus Fixed Physiology

[27] The model assuming the physiological trade-off of OU kinetics agrees significantly better with the data than the model without this trade-off (Table 2). This is particularly evident when the fitted kinetic parameters are plotted versus ambient nitrate concentration (Figure 4). Correlations of the best-fit values of V_{\max} with their corresponding observed values are slightly better for the Affinity model than for the OU model, but the OU model's best-fit values of A are more strongly correlated with the observations by a greater margin (Table 3). Whether the temperature sensitivities of V_{\max} and A were assumed to be the same or distinct made little difference in these correlations for the OU model. In all cases, the ensemble mean values (not shown) of model output (kinetic parameters) were practically indistinguishable from the corresponding best-fit values.

3.4. Combined Effects of Temperature and Concentration

[28] With the Affinity model values of kinetic parameters do not depend on the ambient nitrate concentration (Figure 4), and the inferred temperature sensitivity (E_a/R), is lower than with the OU model (Table 1). The apparent dependence (Figures 4a and 4c) results from the correlation of ambient nitrate concentration and temperature; i.e., at high nitrate concentrations, temperature tends to be low, which results in a tendency for lower V_{\max} and A at high nitrate concentrations.

[29] The differences in inferred temperature sensitivities for the Affinity model versus the OU model result directly from the combined effects of temperature and concentration on the values of V_{\max} and A in the equations of the OU model, in contrast to the dependence of these parameters on only temperature in the Affinity model. In the OU model, V_{\max} increases with both the ambient temperature and ambient nitrate concentration (equation (4)), which means that they tend to have opposing effects, given their negative relationship in this data set (Figure 1) and in the near-surface ocean in general [Silió-Calzada *et al.*, 2008]. This is why the greatest modeled values of V_{\max} with the OU model occur at intermediate values of both nitrate concentration (Figure 4b) and temperature (Figures 2b and 3b), in agreement with the observations. This is also why the inferred sensitivity of V_{\max} is greater for the OU model; i.e., to obtain approximately the same net effect, the temperature sensitivity must be greater in order to counteract the dependence on concentration.

[30] It is surprising, however, that the correlation of the best-fit and observed values of V_{\max} is actually slightly worse for the OU than for the Affinity model (Table 3). There remains considerable room for improvement, given that neither model explains more than about 20% of the variability in V_{\max} .

[31] On the other hand, in the OU model A increases with increasing temperature and with decreasing nitrate concentration (equation (5)). This is why, under the assumption of distinct temperature sensitivities for V_{\max} and A , the inferred

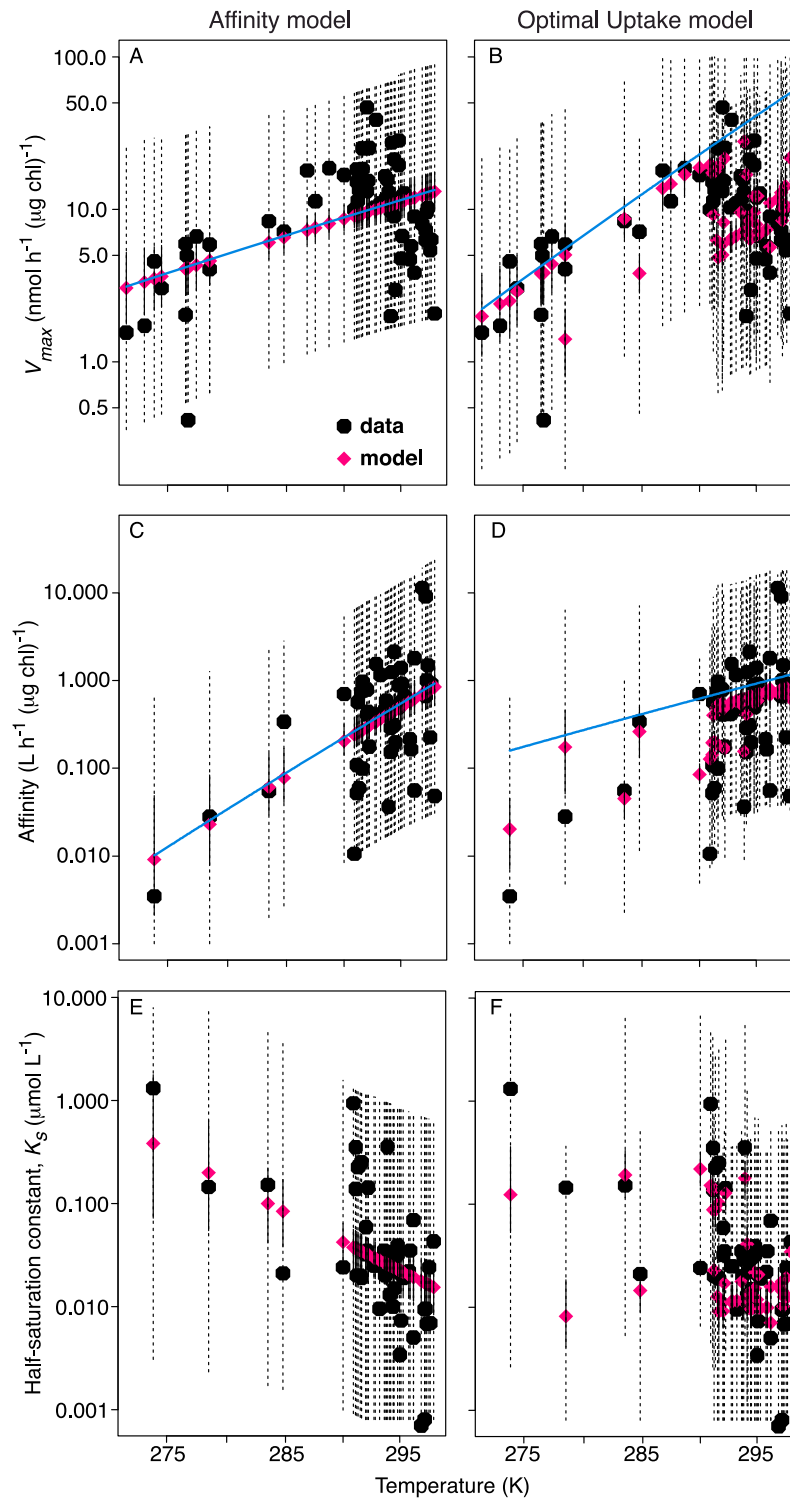


Figure 2. Kinetic parameters for nitrate uptake versus temperature, assuming separate values of temperature sensitivities. Modeled and observed values of maximum uptake rate (V_{max}), affinity (A), and corresponding half-saturation “constants” (K_s). Modeled values of K_s were calculated as V_{max}/A . The two models, respectively, assume either (a, c, e) no physiological trade-off (Affinity model), or (b, d, f) the physiological trade-off specified by the OU model. For each best-fit model value (red diamonds), vertical lines show the 95% quantile range from the ensemble of parameter values (solid lines), and the 95% quantile range of predicted observations, based on the ensemble of standard errors (dotted lines). Solid blue lines show the effect of temperature alone, using the best-fit parameters for each model, respectively. With the Affinity model, modeled values depend only on temperature, but with the OU model they also depend on ambient nutrient concentration (not shown).

Table 1. Results of AM Fits of Equations to the Data^a

Parameter (Units)	Affinity Model	OU Model
<i>Assuming Distinct Temperature Sensitivities for V_{\max} and A</i>		
$V_{\max, r}$ (nmol h ⁻¹ (μ g Chl) ⁻¹)	10.3 (1.12)	-
$V_{0, r}$ (nmol h ⁻¹ (μ g Chl) ⁻¹)	-	32.7 (7.31)
A_r (L h ⁻¹ (μ g Chl) ⁻¹)	0.386 (0.073)	-
$A_{0, r}$ (L h ⁻¹ (μ g Chl) ⁻¹)	-	0.792 (0.180)
$E_{a, V}/R$ (K)	4,470 (1,080)	10,000 (1,580)
$E_{a, A}/R$ (K)	15,300 (3,240)	6,750 (3,500)
Other posterior quantities		
$\sigma_{\log_{10} V_{\max}}$	0.333 (0.032)	0.362 (0.034)
$\sigma_{\log_{10} A}$	0.560 (0.058)	0.514 (0.056)
LL	-73.8	-74.4
AIC	156	157
<i>Assuming the Same Temperature Sensitivity for V_{\max} and A</i>		
$V_{\max, r}$ (nmol h ⁻¹ (μ g Chl) ⁻¹)	10.8 (1.14)	-
$V_{0, r}$ (nmol h ⁻¹ (μ g Chl) ⁻¹)	-	31.2 (6.65)
A_r (L h ⁻¹ (μ g Chl) ⁻¹)	0.378 (0.077)	-
$A_{0, r}$ (L h ⁻¹ (μ g Chl) ⁻¹)	-	0.795 (0.20)
E_a/R (K)	5,440 (1,060)	9,380 (1,250)
Other posterior quantities		
$\sigma_{\log_{10} V_{\max}}$	0.336 (0.031)	0.367 (0.035)
$\sigma_{\log_{10} A}$	0.610 (0.064)	0.508 (0.054)
LL	-72.5	-68.7
AIC	151	144

^aFor kinetic parameters and estimated standard errors (σ , from Gibbs sampling), the mean (standard deviation in parentheses) is reported over the ensemble of 64×10^6 simulations for each model, respectively. Values of rate coefficients are for a reference temperature of 293 K. LL is the ensemble mean log likelihood. Akaike Information Criteria (AIC) [Akaike, 1974] are calculated from equation (8) based on this LL, the number of parameters fitted, and the number of observations.

temperature sensitivity is much greater with the Affinity model than with the OU model; i.e., the higher temperature sensitivity compensates for the lack of dependence of A on ambient nitrate concentration in the Affinity model. The correlations of modeled and observed values of A and K_s , respectively, are greater with the OU model than with the Affinity model, and by a wide margin under the assumption of identical temperature sensitivities for V_{\max} and A (Table 3).

[32] The observed and fitted values of kinetic parameters together with observed ambient nitrate concentration, can be used to estimate the in situ uptake rates at ambient conditions. Although neither model represents the full range of estimated in situ uptake rates, the model accounting for the physiological trade-off (Figure 5b) predicts a slightly wider range of uptake rates, which agrees better with the estimates based on the reported kinetic parameters than does the model without physiological acclimation (Figure 5a). However, there is no difference in the correlations of the estimates based on the Affinity and OU models, respectively, with the estimates based on the observed values of kinetic parameters ($r^2 = 0.51$ for both models, Figure 5). This similarity results from the fact that both models were fitted to the same observations. Although the two models produce similar estimates of in situ uptake rates for the precise values of observed ambient temperature and concentration from this data set, they would produce different results for different ambient conditions, specifically for a different relationship between temperature and concentration than that in this data set.

3.5. Inhibition of Nitrate Uptake by Ammonium

[33] The well known inhibition of nitrate uptake in the presence of ammonium, which was a major focus of the study by Harrison *et al.* [1996], deserves mention as a potential determinant of the overall pattern for V_{\max} . They estimated parameters for this inhibition using incubations with graded additions of isotopically labeled ammonium. As they stated, this does not directly assess the degree of inhibition in situ. Still, it provides the best data to estimate what that effect might be, specifically for this data set. Using the reported values of inhibition parameters together with the in situ ammonium concentration, the mean value of inhibition, expressed as the factor ($0 \leq \gamma \leq 1$) by which maximum nitrate uptake rate would be reduced [Harrison *et al.*, 1996, equation 3], is 0.91 (standard deviation = 0.10, $n = 42$). This suggests that this inhibition plays a minor role in determining the overall pattern for V_{\max} of nitrate uptake. However, these observations are from a relatively iron-replete region, and ammonium inhibition of nitrate is likely to be stronger under iron limitation [Armstrong, 1999].

4. Discussion

4.1. Lack of Temperature Dependence for K_s

[34] Whereas Smith *et al.* [2009] could only present plausible yet somewhat equivocal arguments that the pattern of K_s was more likely determined by pre-acclimation to the ambient nutrient concentration rather than by temperature, the results herein make clear that the explanation in terms of the nutrient concentration is more consistent with the data set as a whole. This validates the implicit assumption of a constant value for the ratio V_0/A_0 as applied by Smith [2010] in analyzing the combined effects of temperature and concentration on V_{\max} only. Although this validates the widely applied assumption that K_s is independent of temperature in models using MM kinetics [Goldman and Carpenter, 1974], the results herein also clearly show that OU kinetics better reproduces the observed variations in kinetic parameters compared to the Affinity model. This finding also explains the robust relationship between K_s and ambient nitrate concentration as observed in compilations of data from diverse studies of uptake rates in both marine and freshwater environments [Collos *et al.*, 2005; Smith *et al.*, 2009]. It thus explains why the prediction of OU kinetics, that K_s should increase as the square root of ambient nutrient concentration, agrees with observations from various environments despite differences in temperature [Smith *et al.*, 2009].

Table 2. Number of Parameters Fitted (p), Akaike Information Criteria (AIC), Difference in AIC (Δ_{AIC}), and the Resulting Akaike Weights (w) From Equation (10), Which Are the Relative Normalized (0, 1) Probabilities for Each of the Four Models Considered

Model	p	AIC	Δ_{AIC}	w
Affinity model, distinct T sensitivities	4	156.0	12.42	0.0020
Affinity model, identical T sensitivities	3	151.2	7.620	0.0216
OU model, distinct T sensitivities	4	157.2	13.64	0.0010
OU model, identical T sensitivities	3	143.6	0	0.9753

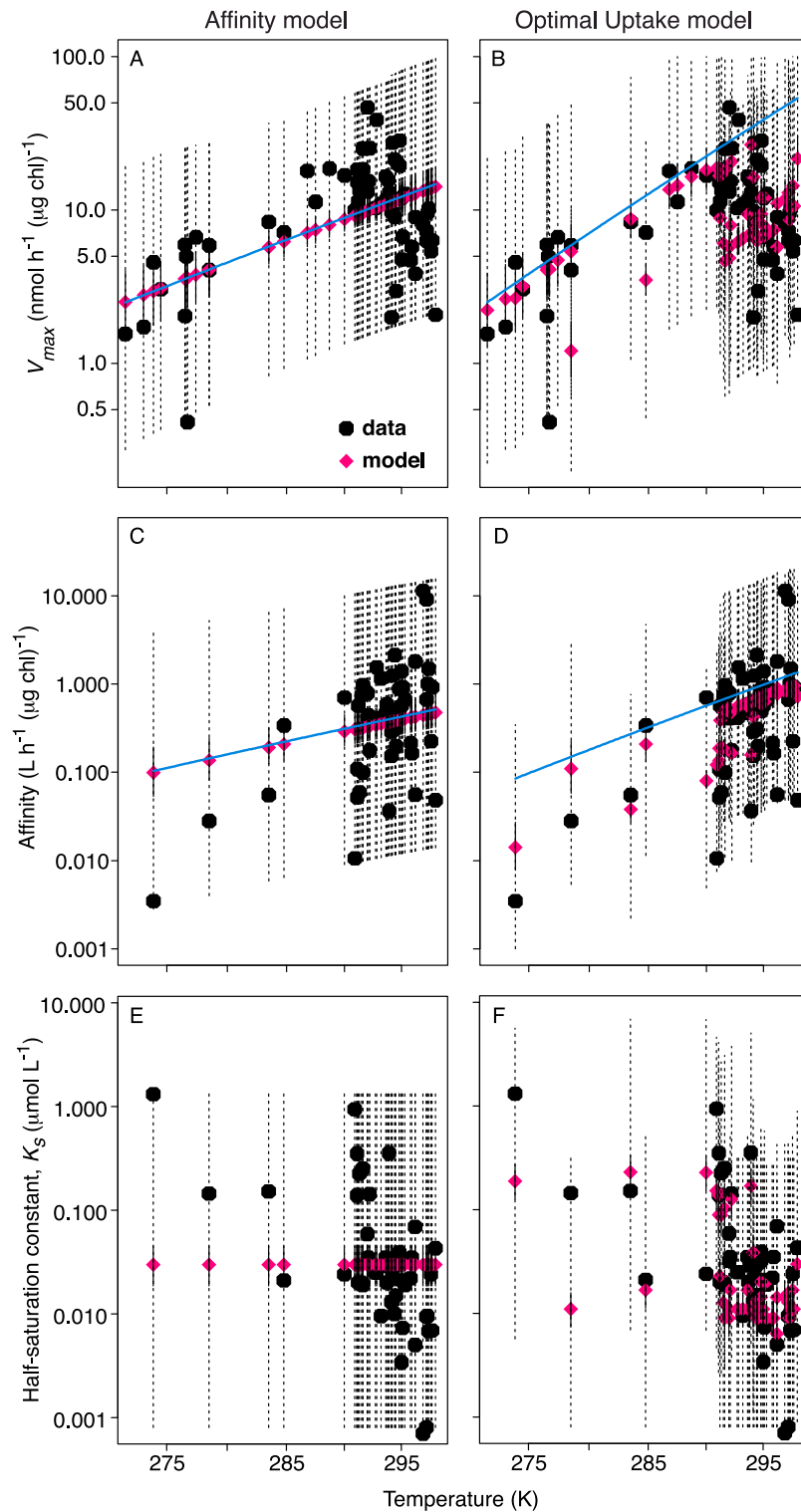


Figure 3. Kinetic parameters for nitrate uptake versus temperature, assuming the same temperature sensitivity for maximum uptake rate and affinity. As in Figure 2, but fits of models were conducted assuming the same temperature sensitivity for V_{\max} and A within each model, respectively.

4.2. Temperature Sensitivity of Uptake Rate

[35] For a simple exponential function such as employed by *Eppley* [1972], the relative increase for a given change in temperature is constant, whereas for the Arrhenius equation

it depends on the specific temperature interval. The former is sometimes given the shorthand ' Q_{10} ', e.g., a Q_{10} of 2 indicates a doubling of rate for a 10 K increase in temperature. Although the increase varies with temperature in the Arrhenius equation, this makes a difference of only about

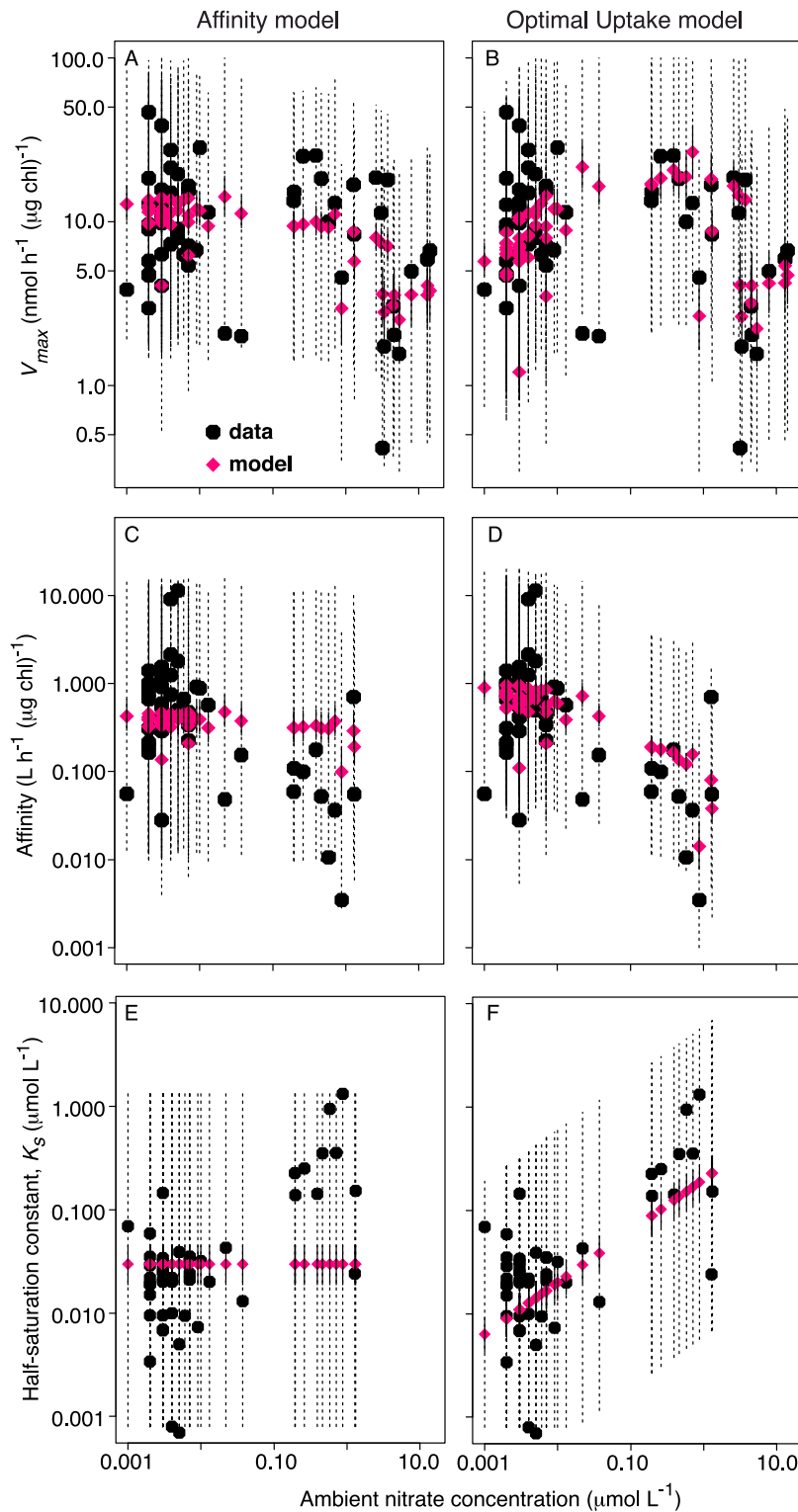


Figure 4. Kinetic parameters for nitrate uptake versus ambient nitrate concentration, assuming the same temperature sensitivity for maximum uptake rate and affinity. As in Figure 2, except plotted versus ambient nitrate concentration.

10% over the range of ambient temperatures in the near-surface ocean. For an increase from 10 to 20°C, the rate increases by 3.1 times for $E_a/R = 9380$ K (Table 1) versus 2.9 times for 20 to 30°C. For E_a estimated for the Affinity model, these values are 1.9 and 1.8 times respectively.

Therefore, the best fits of the Arrhenius function for the two models yield a Q_{10} of ~ 3 and ~ 2 for the OU and Affinity (MM) models, respectively. The latter is indistinguishable from the estimate of Q_{10} for growth [Eppley, 1972; Bissinger *et al.*, 2008] as widely applied for various pro-

Table 3. Correlation Coefficients, r^2 (p-Values in Parentheses) of Best-Fit Model Output With the Corresponding Observations

Observable (Number of Observations)	Affinity Model	OU Model
<i>Assuming Distinct Temperature Sensitivities for V_{\max} and A</i>		
$V_{\max}(N = 60)$	0.22 (2×10^{-4})	0.18 (6×10^{-4})
$A(N = 48)$	0.33 (2×10^{-5})	0.47 (8×10^{-8})
$K_s(N = 48)$	0.35 (1×10^{-5})	0.39 (2×10^{-6})
<i>Assuming the Same Temperature Sensitivity for V_{\max} and A</i>		
$V_{\max}(N = 60)$	0.22 (2×10^{-4})	0.16 (2×10^{-3})
$A(N = 48)$	0.33 (2×10^{-5})	0.47 (7×10^{-8})
$K_s(N = 48)$	0.00 (1)	0.43 (4×10^{-7})

cesses, including uptake, in ecosystem models. This shows that the temperature sensitivity obtained herein with the OU model is considerably greater than that commonly applied in ecosystem models.

[36] The temperature sensitivity inferred based on OU kinetics is at the high end of the typical range of $Q_{10} = 2$ to 3 reported for growth of heterotrophic bacteria [Pomeroy and Wiebe, 2001]. Further studies are needed to test the combined effects of nutrient concentration and temperature on phytoplankton growth rates, which may exhibit complex interactions, given these results for nutrient uptake and the fact that such interactions are well known, although not entirely well understood, for bacteria [Pomeroy and Wiebe, 2001]. Whether there is in general a difference in the temperature sensitivity of autotrophic versus heterotrophic processes will partially determine whether warming of the near-surface ocean will bring about a net increase or

decrease in the rate of export of carbon to the deep ocean [Riebesell *et al.*, 2009].

4.3. Modeling Oceanic Uptake

[37] The findings herein support the hypothesis that the pattern of nitrate uptake in the ocean is largely determined by the physiological trade-off between V_{\max} and A [Smith *et al.*, 2009], in combination with temperature. As in work by Smith [2010]: (1) the caveat applies that biomass-specific rates may be less sensitive to temperature than the chlorophyll-specific rates examined herein, but nevertheless (2) the difference between the inferred temperature sensitivities with the Affinity model versus OU kinetics is an inescapable result of the negative correlation between temperature and nutrient concentration in the near-surface ocean, which will apply even for biomass-specific rates.

[38] For large-scale modeling of the ocean, which generally does not resolve the short time scales of the experiments analyzed herein, the assumption of instantaneous acclimation is appropriate. Substituting the short-term approximations of equations (4) and (5) into equation (2), with $S_a = S$, gives the long-term (acclimated) response [Pahlow, 2005; Smith *et al.*, 2009] for uptake rate:

$$V_{OU} = \frac{V_0 S}{\left(\frac{V_0}{A_0} + 2\sqrt{\frac{V_0 S}{A_0}} + S\right)} \quad (11)$$

5. Conclusions

[39] I find in this data set no evidence that the temperature sensitivities of affinity and maximum uptake rate differ, and

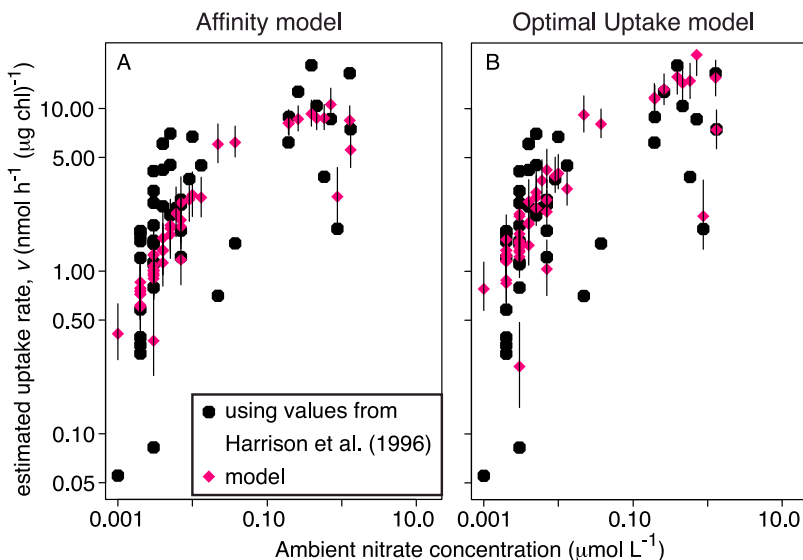


Figure 5. Estimated in situ nitrate uptake rates based on observed ambient nitrate concentrations. Calculated using either reported values of uptake parameters from the ship-board incubations using graded nutrient additions of Harrison *et al.* [1996] (black circles) or the best-fits of models for variation in those parameters (red diamonds) assuming either (a) no physiological trade-off (Affinity model) or (b) the physiological trade-off specified by OU kinetics. Vertical lines show 95% quantile ranges of modeled rates calculated from the ensemble of parameter values. Correlations between the estimated rates from the models and those estimated from the reported kinetic parameters are indistinguishable at $r^2 = 0.51$ ($F = 48.1$ for the Affinity model versus $F = 48.5$ for the OU model; $n = 48$ and $p < 10^{-7}$ for both).

therefore no evidence that half-saturation constants for nitrate uptake should depend on temperature. If this is the case in general, it would explain observations of a robust relationship between half-saturation constants, as fit to the MM equation, and the ambient nutrient concentration [Collos *et al.*, 2005; Smith *et al.*, 2009].

[40] Although OU kinetics agrees better with the data set as a whole than does MM kinetics, there remains considerable room for improvement in the modeling of nitrate uptake kinetics, particularly with respect to the variability in V_{\max} . Further studies are warranted to seek better representations of the physiological trade-off(s) underlying the acclimation and adaptation of phytoplankton to nutrient concentrations.

[41] Large-scale models of planktonic ecosystems and biogeochemical cycles should account explicitly for the combined effects of temperature and physiological acclimation (or evolutionary adaptation) to ambient nutrient concentrations. Smith *et al.* [2009] found that accounting for the physiological trade-off of OU kinetics in an Earth-system climate model made considerable differences in the projected response of marine productivity to global warming, even though they assumed the same temperature sensitivity for both MM and OU kinetics. Such large-scale modeling studies should also explore the use of greater temperature sensitivities for phytoplankton processes. Although the findings herein concern the overall ecological response, not the response for any particular species, they can inform the choice of trait-space and trade-offs in models that do resolve many different species or functional types [Follows and Dutkiewicz, 2011].

[42] **Acknowledgments.** J. D. Annan and J. C. Hagreaves assisted with implementing the Adaptive Metropolis algorithm and interpretation of the results. Y. Yamanaka and A. Oeschlies provided helpful suggestions. This work was supported by the Kakushin project of the Ministry of Education, Culture, Sports, Science and Technology (MEXT) of Japan.

References

- Akaike, H. (1974), A new look at the statistical model identification, *IEEE Trans. Autom. Control*, *19*, 716–723, doi:10.1109/TAC.1974.1100705.
- Aksnes, D. L., and J. K. Egge (1991), A theoretical model for nutrient uptake in phytoplankton, *Mar. Ecol. Prog. Ser.*, *70*, 65–72, doi:10.3354/meps070065.
- Anderson, D. R., K. P. Burnham, and W. L. Thompson (2000), Null hypothesis testing: Problems, prevalence, and an alternative, *J. Wildl. Manage.*, *64*, 912–923.
- Armstrong, R. A. (1999), An optimization-based model of iron-light-ammonium colimitation of nitrate uptake, *Limnol. Oceanogr.*, *44*, 1436–1446, doi:10.4319/lo.1999.44.6.1436.
- Aumont, O., E. Maier-Reimer, S. Blain, and P. Monfray (2003), An ecosystem model of the global ocean including Fe, Si, P colimitations, *Global Biogeochem. Cycles*, *17*(2), 1060, doi:10.1029/2001GB001745.
- Bissinger, J. E., D. J. S. Montagnes, J. Sharples, and D. Atkinson (2008), Predicting marine phytoplankton maximum growth rates from temperature: Improving on the Eppley curve using quantile regression, *Limnol. Oceanogr.*, *53*, 487–493.
- Burnham, K. P., and D. R. Anderson (1998), *Model Selection and Inference: A Practical Information-Theoretic Approach*, Springer, New York.
- Carlin, B. P., and T. A. Louis (1996), *Bayes and Empirical Bayes Methods for Data Analysis*, 1st ed., *Monogr. Stat. Appl. Probab.*, vol. 69, Chapman and Hall, London.
- Collos, Y., A. Vaquer, and P. Souchu (2005), Acclimation of nitrate uptake by phytoplankton to high substrate levels, *J. Phycol.*, *41*, 466–478, doi:10.1111/j.1529-8817.2005.00067.x.
- Congdon, P. (2001), *Bayesian Statistical Modelling*, John Wiley, Chichester, U. K.
- Dauta, A. (1982), Conditions for phytoplankton development, comparative study of the behaviour of eight species in culture. II. Role of nutrients: Assimilation and intracellular storage, *Ann. Limnol.*, *18*, 263–292, doi:10.1051/limn/1982014.
- Dugdale, R. C. (1967), Nutrient limitation in the sea: Dynamics, identification, and significance, *Limnol. Oceanogr.*, *12*, 685–695.
- Eppley, R. W. (1972), Temperature and phytoplankton growth in the sea, *Fish. Bull.*, *70*, 1063–1085.
- Eppley, R. W., J. N. Rogers, and J. J. McCarthy (1969), Half-saturation constants for uptake of nitrate and ammonium by marine phytoplankton, *Limnol. Oceanogr.*, *14*, 912–920.
- Fasham, M. J. R., J. L. Sarmiento, R. D. Slater, H. W. Ducklow, and R. Williams (1993), Ecosystem behaviour at Bermuda station “S” and ocean weather station “India”: A general circulation model and observational analysis, *Global Biogeochem. Cycles*, *7*, 379–415, doi:10.1029/92GB02784.
- Follows, M. J., and S. Dutkiewicz (2011), Modeling diverse communities of marine microbes, *Annu. Rev. Mar. Sci.*, *3*, 427–451, doi:10.1146/annurev-marine-120709-142848.
- Follows, M. J., S. Dutkiewicz, S. Grant, and S. W. Chisholm (2007), Emergent biogeography of microbial communities in a model ocean, *Science*, *315*, 1843–1846, doi:10.1126/science.1138544.
- Gelman, A., J. B. Carlin, H. S. Stern, and D. B. Rubin (2004), *Bayesian Data Analysis*, 2nd ed., Chapman and Hall, Boca Raton, Fla.
- Gentle, J. E. (2003), *Random Number Generation and Monte Carlo Methods*, 2nd ed., Springer, New York.
- Goldman, J. C., and E. J. Carpenter (1974), A kinetic approach to the effect of temperature on algal growth, *Limnol. Oceanogr.*, *19*, 756–766.
- Haario, H., E. Saksman, and J. Tamminen (2001), An adaptive Metropolis algorithm, *Bernoulli*, *7*, 223–242.
- Harrison, P. J., J. S. Parslow, and H. L. Conway (1989), Determination of nutrient uptake kinetic parameters: A comparison of methods, *Mar. Ecol. Prog. Ser.*, *52*, 301–312.
- Harrison, W. G., L. R. Harris, and D. B. Irwin (1996), The kinetics of nitrogen utilization in the oceanic mixed layer: Nitrate and ammonium interactions at nanomolar concentrations, *Limnol. Oceanogr.*, *41*, 16–32.
- Healey, F. P. (1980), Slope of the Monod equation as an indicator of advantage in nutrient competition, *Microb. Ecol.*, *5*, 281–286, doi:10.1007/BF02020335.
- Healy, M. (1968a), Algorithm AS 7: Inversion of a positive semi-definite matrix, *Appl. Stat.*, *17*, 198–199.
- Healy, M. (1968b), Algorithm AS 6: Triangular decomposition of a symmetric matrix, *Appl. Stat.*, *17*, 195–197.
- Kanda, J., T. Saino, and A. Hattori (1985), Nitrogen uptake by natural populations of phytoplankton and primary production in the Pacific Ocean: Regional variability of uptake capacity, *Limnol. Oceanogr.*, *30*, 987–999.
- Kishi, M. J., et al. (2007), NEMURO—A lower trophic level model for the North Pacific marine ecosystem, *Ecol. Modell.*, *202*, 12–25.
- Laine, M. (2008), Adaptive MCMC methods with applications in environmental and geophysical models, Ph.D. thesis, Lappeenranta Univ. of Technol., Lappeenranta, Finland.
- LeQuere, C., et al. (2005), Ecosystem dynamics based on plankton functional types for global ocean biogeochemistry models, *Global Change Biol.*, *11*, 2016–2040, doi:10.1111/j.1365-2486.2005.1004.x.
- Marinov, I., M. Follows, A. Gnanadesikan, J. L. Sarmiento, and R. D. Slater (2008), How does ocean biology affect atmospheric $p\text{CO}_2$? Theory and models, *J. Geophys. Res.*, *113*, C07032, doi:10.1029/2007JC004598.
- Moisan, J. R., T. A. Moisan, and M. R. Abbott (2002), Modelling the effect of temperature on the maximum growth rates of phytoplankton populations, *Ecol. Modell.*, *153*, 197–215, doi:10.1016/S0304-3800(02)00008-X.
- Pahlow, M. (2005), Linking chlorophyll-nutrient dynamic to the Redfield N:C ratio with a model of optimal phytoplankton growth, *Mar. Ecol. Prog. Ser.*, *287*, 33–43.
- Parekh, P., M. J. Follows, and E. A. Boyle (2005), Decoupling of iron and phosphate in the global ocean, *Global Biogeochem. Cycles*, *19*, GB2020, doi:10.1029/2004GB002280.
- Pomeroy, L. R., and W. J. Wiebe (2001), Temperature and substrates as interactive limiting factors for marine heterotrophic bacteria, *Aquat. Microb. Ecol.*, *23*, 187–204, doi:10.3354/ame023187.
- Riebesell, U., A. Körtzinger, and A. Oeschlies (2009), Sensitivities of marine carbon fluxes to ocean change, *Proc. Natl. Acad. Sci. U. S. A.*, *109*, 20,602–20,609, doi:10.1073/pnas.0813291106.
- Schwarz, G. E. (1978), Estimating the dimension of a model, *Ann. Stat.*, *6*, 461–464.
- Silió-Calzada, A., A. Bricaud, and B. Gentili (2008), Estimates of sea surface nitrate concentrations from sea surface temperature and chlorophyll concentration in upwelling areas: A case study for the Benguela system, *Remote Sens. Environ.*, *112*, 3173–3180, doi:10.1016/j.rse.2008.03.014.

Smith, S. L. (2010), Untangling the uncertainties about combined effects of temperature and concentration on nutrient uptake rates in the ocean, *Geophys. Res. Lett.*, *37*, L11603, doi:10.1029/2010GL043617.

Smith, S. L., Y. Yamanaka, M. Pahlow, and A. Oschlies (2009), Optimal uptake kinetics: Physiological acclimation explains the pattern of nitrate uptake by phytoplankton in the ocean, *Mar. Ecol. Prog. Ser.*, *384*, 1–12, doi:10.3354/meps08022.

Yamanaka, Y., and E. Tajika (1996), The role of the vertical fluxes of particulate organic matter and calcite in the oceanic carbon cycle: Stud-

ies using an ocean biogeochemical general circulation model, *Global Biogeochem. Cycles*, *10*, 361–382, doi:10.1029/96GB00634.

S. L. Smith, Environmental Biogeochemical Cycles Research Program, RIGC, JAMSTEC, 3173-25 Showa-machi, Kanazawa-ku, Yokohama-shi, Kanagawa-ken 236-0001, Japan. (lanimal@jamstec.go.jp)